4*d* photoionization and subsequent Auger decay in atomic Eu

A. Sankari,[1,*] R. Sankari,[2] S. Heinäsmäki,[1] M. Huttula,[1] S. Aksela,[1] and H. Aksela[1]
[1]*Department of Physical Sciences, University of Oulu, P.O. Box 3000, 90014 Oulu, Finland*
[2]*Department of Physics, University of Turku, 20014 Turku, Finland*
(Received 20 February 2008; published 5 May 2008)

The synchrotron-radiation-excited 4*d* photoelectron and subsequent Auger spectra of atomic Eu have been recorded with high resolution. The lifetime widths, intensity ratios, and binding energies of the most prominent ^9D states of the $4d^{-1}$ configuration have been determined with high accuracy from the measured spectrum. Experimental spectra have been compared with the results of relativistic multiconfiguration Dirac-Fock calculations. The features seen in the Auger spectrum have been found to be predominantly due to Coster-Kronig and super-Coster-Kronig transitions.

DOI: 10.1103/PhysRevA.77.052703 PACS number(s): 32.80.Hd, 32.80.Fb

I. INTRODUCTION

The study of the electronic and magnetic structure of europium as well as other rare-earth elements is motivated by their present and future industrial applications. Deep understanding of the phenomena behind useful techniques and further development of new applications is preceded by a careful investigation of the properties and dynamics of the electronic structure of elements. For this task, electron spectroscopy is a competent tool in the study of the electronic and magnetic properties of atoms, molecules, and solids.

Third-generation synchrotron light sources provide sufficient flux to study metal vapors with high resolution. Extensive simulations are required in the interpretation of experimental high-resolution electron spectra. However, rare-earth elements with their open 4*f* shell still offer challenges from the computational point of view, despite the increased computer power.

In case of Eu, the half-filled 4*f* shell facilitates slightly the computations and therefore it has been studied widely both experimentally and theoretically. Various theoretical approaches have been applied to explain the experimentally observed features in photoabsorption spectra: the random-phase approximation with exchange (RPAE) [1] and the many-body perturbation theory (MBPT) [2] to name a few. Also the Hartree-Fock method has been successful in predicting the features seen in the 5*p* [3] and 4*d* photoelectron spectra [4,5] of Eu.

Recently [6], the relativistic multiconfiguration Dirac-Fock (MCDF) method was applied to the 3*p* photoelectron and subsequent Auger electron spectra of atomic manganese with a half-filled 3*d* shell. It was found that a single-configuration calculation was enough to reproduce the main features of the photoelectron spectrum, whereas the following Auger decay proved to be much more sensitive for the approximation used.

To further test the predictions of the multiconfiguration Dirac-Fock theory in a similar but more demanding situation, the 4*d* photoemission and subsequent Auger decay of atomic europium is studied in this work. The 4*d* photoelectron spectrum of Eu was studied earlier by Gerth *et al.* experimentally [5]. They presented also a calculated spectrum and lifetime widths using the Hartree-Fock approximation. Luhmann *et al.* [7] have also studied photoelectrons from the valence to the 4*d* shell in coincidence with photo-ions, providing detailed information about the charge state of the final ions.

There are only a few studies of Auger decay following 4*d* ionization in atomic Eu. Kukk *et al.* [8] studied the resonant Auger spectrum below, at, and above the giant $4d \rightarrow 4f$ resonance, whereas Santjer *et al.* [9] used electron excitation in their study, which resulted in more complicated spectral features to analyze. According to our knowledge, the only synchrotron-radiation-excited Auger spectrum well above the giant resonance, but below the 4*p* threshold, has been measured by Sairanen and Aksela for solid Eu [10]. In the present work, also the 4*d* Auger spectrum of atomic Eu is studied experimentally and the observed features are interpreted with the help of MCDF calculations.

II. EXPERIMENT

The experimental data for this work were obtained at the gas-phase beamline I411 at the third-generation storage ring MAX-II in Lund, Sweden [11]. The atomic vapor of Eu was produced by an oven heated either resistively or by induction (ovens are described in Refs. [12,13]). The temperature, measured by a thermocouple, was about 600 °C. A modified rotatable hemispherical SES-100 analyzer [12] set in the 1-m section of the beamline was used to analyze the kinetic energies of the electrons. The spectrometer was rotated to an angle of 54.7° with respect to the polarization vector of incoming radiation.

The 4*d* photoelectron spectrum (shown in the upper panel of Fig. 1) was measured at a photon energy of 310 eV and a constant pass energy of 100 eV. The monochromator exit slit was set to 50 μm. The energy region of the most prominent 4*d* photolines (in the middle panel of Fig. 1) was measured with a photon energy of 165 eV and a 20-eV pass energy in order to achieve higher resolution. With a monochromator exit slit of 40 μm, a resulting overall experimental resolution of 105 meV was obtained; this value was confirmed by measuring the Xe 5*p* photolines. Doppler broadening, about

*anna.sankari@oulu.fi

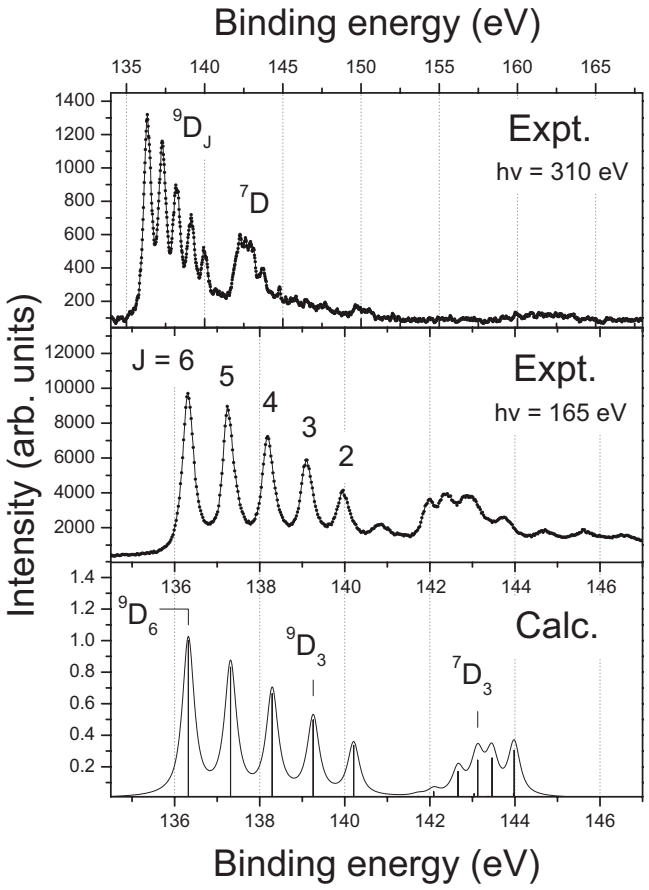

FIG. 1. Experimental 4*d* photoelectron spectrum measured with a photon energy of 310 eV (upper panel). The middle panel shows the most prominent 4*d* photolines measured with a photon energy of 165 eV. The lower panel shows our calculation, which has been shifted to correspond to the experimental energies, as well as the selected initial ionic states used in the calculation of the Auger transition rates. The calculated line spectrum was convolved with the experimental Gaussian broadening of 0.1 eV and with a Lorentzian contribution of 0.3 eV.

20 meV [14], was also taken into account in the analysis of the Eu spectrum. This information allowed us to determine the Lorentzian type of broadening—i.e., the lifetime widths of the most prominent 4*d* photolines from the spectrum shown in Fig. 1. The determined lifetime widths are given in Table I together with the relative intensities and binding energies of the ^9D quintet. The accuracy of the experimental energies is about 5 meV, whereas the lifetime widths have error limits of 30 meV.

Both the photon and binding energy calibrations were made using the well-known binding energies of the Xe 4*d* photolines [15] as well as the kinetic energies of the subsequent $N_{4,5}O_{2,3}O_{2,3}$ Auger lines [16]. The 4*d* photolines and subsequent Auger lines of xenon measured with different photon energies were also used in the transmission correction as described in Ref. [17].

The Auger spectrum of Eu shown in the upper panel of Fig. 2 was recorded using a 50-eV pass energy and 165-eV photon energy. As a result, the energy resolution was about 190 ± 10 meV, which is better than in the 4*d* photoelectron spectrum shown in the upper panel of Fig. 1. Due to the open-shell structure of Eu, the 4*d* photoelectron spectrum and the subsequent Auger decay spectrum are spread over an energy range of tens of eV. Combined with the fact that the photon flux at beamline I411 decreases gradually above the 140-eV photon energy, the lowest possible photon energy above the $4d^{-1}$ states (165 eV) was chosen. As a result, the Auger decay spectrum was located between the 4*d* and the overlapping 5*s* and 5*p* photolines. However, the 5*s* and 5*p* photoelectron lines are also widely spread in energy and the high-kinetic-energy part of the Auger spectrum overlapped with the 5*s* and 5*p* photolines as can be seen from the upper panel of Fig. 2 (solid line). With higher photon energies (>195 eV), the 4*d* photoelectron spectrum started to overlap with the low-kinetic-energy part of the Auger spectrum. On the other hand, measurements with photon energies above 300 eV, which would have moved the 4*d* photolines above the Auger decay spectrum, would also have ionized the 4*p* orbitals, complicating the situation even more.

In order to subtract the photolines from the Auger spectrum, additional measurements were performed. The Auger spectrum was measured with several photon energies: 165 eV, 180 eV, and 195 eV. Together with a pure 5*s* and 5*p* photoelectron spectra, measured with a photon energy of 80 eV, the photolines were subtracted from the transmission corrected Auger spectrum. The resulting spectrum is shown in the upper panel of Fig. 2 (dashed line).

TABLE I. Binding energies (in eV), intensities with respect to the $^9D_6$ state, and natural lifetime widths (in eV) of the $4d^{-1}$ ^9D states of atomic Eu. Calculated energies have been shifted to correspond to the experimental energy of the $^9D_6$ state.

	This work					Ref. [5]			
	Expt.			Calculated		Expt.	Calculated		
State	E_B	Intensity	Γ_L	E_B	Intensity	E_B	E_B	Intensity	Γ_L
$^9D_6$	136.322	1.000	0.27	136.32	1.000	136.32	136.32	1.000	0.17
$^9D_5$	137.261	0.927	0.31	137.32	0.831	137.26	137.20	0.820	0.18
$^9D_4$	138.203	0.713	0.33	138.29	0.663	138.19	138.07	0.642	0.17
$^9D_3$	139.113	0.528	0.35	139.26	0.497	139.08	138.93	0.472	0.21
$^9D_2$	139.957	0.366	0.41	140.21	0.336	139.89	139.77	0.296	0.23

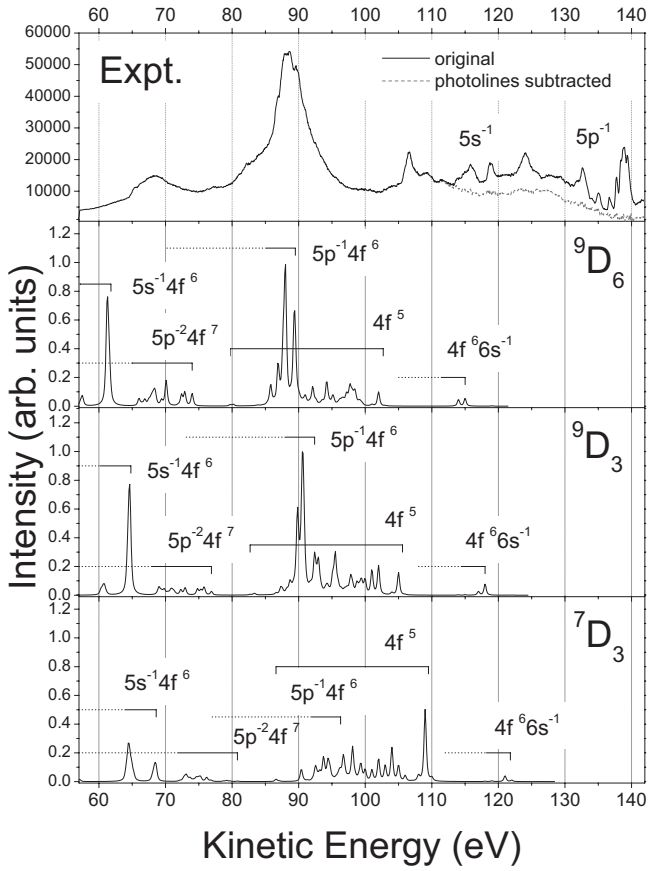

FIG. 2. Experimental 4*d* Auger spectrum (upper panel) together with 5*s* and 5*p* photolines (solid line) and a sketch of the result without photolines (dashed line). The calculated spectra from the $^9D_6$, $^9D_3$, and $^7D_3$ states are also shown (see text for details).

III. THEORY

The wave functions and energies for the ground, initial ionic, and final ionic states of Eu were obtained using the relativistic atomic structure package GRASP92 [18]. In the ground-state configuration $[Xe]4f^76s^2$ the lowest energy level ($^8S_{7/2}$ in *LS* coupling) is 1.6 eV below the first excited state [19], which is not thermally populated in the temperatures used. Therefore an optimal level (OL) calculation was performed to obtain only the energy for the lowest level in the ground state.

In the initial ionic state ($4d^{-1}4f^7$) an extended optimal level (EOL) calculation was utilized to obtain wave functions and energies for 60 lowest levels. Applying the same method used in Refs. [6,20], the ionization probability was estimated by the weights of the ground-state configurations $[Xe]4f^76s^2(^8S_{7/2})$ in the initial ionic states in the frozen-core approximation, which gave the relative intensities after multiplication with an angular-momentum-dependent weight factor. The calculated photoelectron spectrum obtained using this approximation is shown in the lower panel of Fig. 1.

The Auger decay following the photoionization of a 4*d* electron was treated as a simplified two-step process independent of the ionization process. This deexcitation process results in two holes in the outer shells—i.e., $[5s^25p^64f^76s^2]^{-2}$. Accounting for all states belonging to the $5s^{-2}4f^7$, $5s^{-1}5p^{-1}4f^7$, $5s^{-1}4f^6$, $5s^{-1}4f^76s^{-1}$, $5p^{-2}4f^7$, $5p^{-1}4f^6$, $5p^{-1}4f^76s^{-1}$, $4f^5$, $4f^66s^{-1}$, and $4f^76s^{-2}$ configurations would mean a calculation of thousands of states. The EOL calculations performed for some of the Auger final ionic states turned out to be too heavy for our computational resources. Thus only some of the lowest states were calculated from each configuration in single-configuration approximation. In case of Mn [6], mainly the lowest levels of each configuration were populated in the Auger decay which justifies the choice.

The simplest case of the Auger final ionic states, the coupling of five 4*f* electrons with the other closed shells, results in only 198 states, and we calculated all states reached with continuum waves with $j<9/2$ (that is, final ionic states with $J<19/2$), a total of 189 states. In the other extreme, two holes in the 5*p* shell being coupled with seven 4*f* electrons leads to over 4000 states alone. Table II lists the number of final ionic states calculated as well as the number of all possible states. For example, 189 states out of 198 states were calculated for the $4f^5$ configuration and 32 lowest states out of 1695 states were computed for the $5p^{-1}4f^6$ configuration.

The Auger rate calculations proved to be very time consuming, and they were reduced to include only three initial states: from the most prominent quintet the $^9D_6$ and $^9D_3$ states were selected, and from the next multiplet the $^7D_3$ state was chosen because it has a different spin, but the same *J* as the $^9D_3$ state. Continuum waves up to εf orbitals were included, reducing the number of calculated transitions from the number of states as indicated in the third and fourth columns of Table II. Fluorescence decay of the $4d^{-1}$ state has been shown to be negligible [7] and was omitted in the calculations. Table II includes also an averaged transition rate for each initial state and each configuration calculated from the sum of all transitions in a particular configuration by dividing with the number of the transitions (columns 5–7).

Figure 2 shows also the calculated Auger spectrum for each selected initial ionic state. The calculated transition rates have been multiplied by the experimental intensity ratios (1.000, 0.528, and 0.357 for the $^9D_6$, $^9D_3$, and $^7D_3$ states, respectively) and convoluted with a Gaussian broadening of 0.19 eV (the experimental broadening determined from the Xe $N_{4,5}O_{2,3}O_{2,3}$ Auger spectrum) and a Lorentzian contribution of 0.3 eV. The intensity of the $^7D_3$ state was evaluated from the spectrum shown in the middle of Fig. 1, but the results for the ^7D states were omitted from Table I due to larger uncertainties.

IV. RESULTS AND DISCUSSION

A. 4*d* photoelectron spectrum

Table I summarizes the results obtained from the experimental 4*d* photoelectron spectrum shown in Fig. 1 and calculations together with the results given by Gerth *et al.* [5]. The *LS* symbols (obtained by an *LS* conversion) have been used for the states to ease the comparison, although our calculations have been done in *jj*-coupling scheme. In addition, the *LS* terms describe the states better since the *jj*-coupled $4d^{-1}$ states are heavily mixed.

TABLE II. Calculated Auger rates for each final-state configuration. The second column lists how many final ionic states were calculated out of the total number of these states. The third and fourth columns show how many Auger transitions were computed from the initial ionic states with $J=6$ or 3. In addition, an average transition rate (in 10^{-6} a.u.) for each configuration is shown for the $^9D_6$, $^9D_3$, and $^7D_3$ states. The last line shows the sum of calculated states out of all states, number of calculated transitions, and the total sum of the calculated transition rates for each initial ionic state (in eV).

		Transitions from		Initial ionic state		
Final-state configuration	Calculated (all) final ionic states	$J=6$	$J=3$	$^9D_6$	$^9D_3$	$^7D_3$
$4f^5$	189 (198)	158	164	5.2	15.2	23.0
$5s^{-1}4f^6$	30 (576)	22	26	30.0	50.2	44.7
$5p^{-1}4f^6$	32 (1695)	24	31	59.2	79.7	29.2
$4f^6 6s^{-1}$	20 (576)	12	20	5.0	6.2	4.8
$5s^{-2}4f^7$	18 (327)	12	15	57.1	42.5	35.9
$5s^{-1}5p^{-1}4f^7$	20 (3808)	19	16	18.0	15.3	6.4
$5s^{-1}4f^7 6s^{-1}$	30 (1291)	22	23	3.3	2.8	1.6
$5p^{-2}4f^7$	80 (4724)	63	67	6.7	6.8	5.8
$5p^{-1}4f^7 6s^{-1}$	30 (3808)	28	24	1.9	2.0	1.1
$4f^7 6s^{-2}$	30 (327)	17	22	0.1	0.1	0.1
Σ	479 (17330)	377	408	0.123	0.214	0.191

As can be seen from the calculated photoelectron spectrum (plotted in the lower panel of Fig. 1), the main features are reproduced very well by our rough approximative calculation, which did not give any contribution to higher levels analogously with Mn [6]. Taking higher configurations into account would most probably reduce the slightly larger energy splittings in the theoretical line spectrum and divide the intensity to other levels via mixing. It is interesting to note that our approximative intensities are nearly the same as the ones predicted in Ref. [5].

In the earlier study of the $4d$ photoelectron spectrum [5], the only experimental values reported were the binding energies, which are in good accordance with our experimental values. The energy splittings obtained from the Hartree-Fock calculations [5] are slightly closer to the experimental values, reflecting the effects of reduced Slater integrals. We were unable to calculate the lifetime widths for these states, but the computations performed in Ref. [5] gave smaller values than our experimental ones and do not reproduce the clear tendency seen in the experimental lifetime widths, where the width increases as the value of J decreases for the ^9D states.

According to our calculations (cf. Table II), Auger transition rates from the $^9D_3$ state are larger than from the $^7D_3$ state. This would imply smaller lifetime widths for the ^7D multiplet. On the other hand, Gerth *et al.* [5] predicted equal lifetime widths for both $^9D_3$ and $^7D_3$ states. Since our results are merely indicative with a limited number of transitions included, we cannot deduce the tendency of the calculated lifetime widths predicted by a complete set of relativistic calculations. In addition, the energy separations of these lines are too small to separate experimentally (or say even how many lines there are), so this cannot be resolved from the measured spectrum.

B. 4*d* Auger spectrum

In case of Mn [6], the Auger spectrum proved to be very sensitive to different approximations used in the calculations especially of the initial ionic state. The single-configuration approximation overestimated the contribution of the super-Coster-Kronig transitions (which are completely forbidden in the *LS*-coupling scheme for the most prominent multiplet) whereas the inclusion of configuration mixing in the multiconfiguration calculation reduced the transition rates to correspond the experimentally observed spectrum. Unfortunately, it was not possible to perform multiconfiguration calculations for the Auger final ionic states in Eu. Nonetheless, the overestimation of the *LS*-forbidden super-Coster-Kronig transitions to the $4f^5$ states by our single-configuration calculation can be seen from Table II and from Fig. 2, especially for the $^9D_3$ state. The kinetic energies of the super-Coster-Kronig transitions are around 100 eV where in the experimental spectrum there exists a clear dip.

An interpretation of the $4d$ Auger spectrum is complicated because the possible initial ionic states are distributed over a wide energy range and the numerous final-state configurations, also spread widely in energy, overlap with each other as can be seen from the energy diagram obtained from the Hartree-Fock calculations in Ref. [7] as well as from Fig. 2. In addition, except for $4f^7 6s^{-2}$ and $4f^6 6s^{-1}$ configurations, which are hardly populated at all according to our calculations or the ones by Kochur *et al.* [21], the higher part of the $4f^5$ states and all the other configurations are above the third ionization limit and thus may decay further by Auger emission. This broadens the lines even more and smears out any sharp features in the spectrum. The coincidence study by Luhmann *et al.* [7] showed that $4d$ ionization results in mostly triply charged ions, confirming thus the assumption

of at least two subsequent Auger decays. The omission of the lifetime width of the first-step Auger final states is evident from the calculated spectra in Fig. 2 which produced too sharp features when compared to the experimental spectrum.

The strongest feature, the broad strong peak around the kinetic energy of 88 eV, has already earlier [10,22] been attributed to Coster-Kronig transitions to the $5p^{-1}4f^6$ states. This is confirmed by our computations as well as those by Kochur *et al.* [21]. For the ^9D states, the dominant deexcitation pathway is this Coster-Kronig decay, and since the ^9D states are the most populated in the photoionization process, they are also responsible for the strongest features in the subsequent Auger spectrum.

For the ^7D states, the super-Coster-Kronig decay is allowed in the *LS*-coupling scheme and the corresponding branching ratio has been estimated to be about 65% by Kochur *et al.* [21] and McGuire [23] (see Table 18 in Ref. [22]). As pointed out by Kukk *et al.* [8], in the *jj*-coupling scheme already the initial state ($4d^{-1}$) is heavily mixed and the spins of 4*f* electrons are no longer aligned. Consequently, the super-Coster-Kronig transitions are not forbidden, but they are not favored as much as in nonrelativistic calculations (such as those by Kochur *et al.* [21] and McGuire [23]). Inspection of the high-resolution experimental spectrum (see Fig. 2) shows that the contributions from the transitions to the $4f^5$ states are indeed rather weak in comparison with the Coster-Kronig transitions to the $5p^{-1}4f^6$ states in accordance with our calculations. However, the comparison of the calculated Auger spectra from the $^9D_3$ and $^7D_3$ states reveals that the super-Coster-Kronig transitions are more pronounced for the $^7D_3$ state than for the $^9D_3$ state.

Previous experimental works [9,10,22] have attributed the structure around 68 eV to Auger transitions to the $5p^{-2}4f^7$ states. However, these states overlap with the $5s^{-1}4f^6$ and $5s^{-1}4f^76s^{-1}$ states, and according to calculations (see Table II as well as Refs. [21,22]), the most prominent transitions at these kinetic energies would be to the $5s^{-1}4f^6$ states. The kinetic energies of our calculated transitions to the $5s^{-1}4f^6$ states are shifted toward lower energies with respect to the experimental values. In case of Xe, however, the 5*s* hole mixes heavily with the $5p^{-2}5d$ states and this mixing results in a large energy shift and redistribution of intensities [24] as well as changes in the angular distribution of the 5*s* electrons [25]. According to our MCDF calculations, at least the $5s^{-1}4f^7$ and $4f^55d$ configurations of Eu mix, but the calculation together with the $5p^{-2}4f^75d$ configuration turned out to be too heavy. Nonetheless, the mixing of the $5s^{-1}4f^7$ and $4f^55d$ configurations implies that also the $5s^{-1}4f^6$ configuration mixes (at least with the $4f^45d$ configuration) and the corresponding energies are only indicative. This is supported also by the fact that the calculated binding energies of the $5s^{-1}4f^7$ states were too large compared to the experiment. Thus, we state that the feature seen around 68 eV is mostly due to the $4d^{-1}\rightarrow 5s^{-1}4f^6$ transitions with a background produced by $4d^{-1}\rightarrow 5p^{-2}4f^7$ transitions.

Above kinetic energies of 100 eV, the emission of a second-step Auger electron is no longer energetically possible and the Auger final ionic states in this energy region are the $4f^5$, $4f^66s^{-1}$, and $4f^76s^{-2}$ states. The only sharp feature in the Auger spectrum (near $E_K=106$ eV) comes most probably from the super-Coster-Kronig decay of the ^7D multiplet as can be deduced from the calculated spectra in Fig. 2. The contribution of the ^9D states is very modest at this energy range with respect to the ^7D states (cf. calculated transitions rates in Fig. 2).

The reduction of the 5*s* and 5*p* photolines revealed also a hump with kinetic energies over 120 eV. According to our calculations as well as the energy diagram represented by Luhmann *et al.* [7], this could originate from transitions to the lowest configurations—i.e., to the $4f^76s^{-2}$ and $4f^66s^{-1}$ states. The transitions to the latter states would be more probable due to the large overlap between the 4*d* and 4*f* orbitals, but our calculations underestimate the intensity when comparing the prediction to the measured spectra.

In light of the above discussion, the strongest features seen in the Auger decay spectrum following the 4*d* ionization in atomic Eu can be attributed to Coster-Kronig or super-Coster-Kronig transitions involving a 4*f* electron (electrons) in the decay. This is also supported by the Hartree-Fock calculations by Kochur *et al.* [21]. Besides, this is in accordance with the observations from Xe, for which the Coster-Kronig transitions have been found to dominate whenever they are energetically possible [26].

V. CONCLUSIONS

In conclusion, we have measured both the 4*d* photoelectron and the subsequent Auger electron spectra with high resolution. MCDF calculations were performed in order to interpret the structures seen in the measured spectrum. However, even the single-configuration calculations for the Auger final states turned out to be very demanding for our computational resources and we were unable to calculate the lifetime widths of the ^9D components in the 4*d* photoelectron spectrum. Therefore, a comparison with the lifetime widths determined from the experimental spectrum was not possible. Even though we were not able to calculate all of the possible Auger transitions, we confined the calculations to only some of the lowest states of each configurations. With the help of the performed calculations, we were able to identify the structures resolved in the 4*d* Auger spectrum. The most prominent feature around $E_K=88$ eV is attributed to the Coster-Kronig transitions to the $5p^{-1}4f^6$ states and the structure near $E_K=68$ eV to the Coster-Kronig transitions to the $5s^{-1}4f^6$ states. The latter structure has earlier been attributed to Auger transitions to the $5p^{-2}4f^7$ states [9,10,22]. The peak around $E_K=106$ eV results from the super-Coster-Kronig transitions $4d^{-1}\rightarrow 4f^5$, and the broad structure above $E_K=120$ eV is most probably due to the Coster-Kronig decay $4d^{-1}\rightarrow 4f^66s^{-1}$.

ACKNOWLEDGMENTS

The assistance of the MAX-lab staff is acknowledged. This work has been supported by the Finnish Academy for Natural Sciences, National Graduate School in Materials Physics (NGSMP), and by the European Community, Access to Research Infrastructure action of the Improving Human Potential Programme.

[1] M. Ya. Amusia, L. V. Chernysheva, and V. K. Ivanov, Radiat. Phys. Chem. **59**, 137 (2000).
[2] C. Pan, S. L. Carter, and H. P. Kelly, J. Phys. B **20**, L335 (1987).
[3] M. Martins, K. Godehusen, Ch. Gerth, P. Zimmermann, J. Schulz, Ph. Wernet, and B. Sonntag, Phys. Rev. A **65**, 030701(R) (2002).
[4] H. Ogasawara, A. Kotani, and B. T. Thole, Phys. Rev. B **50**, 12332 (1994).
[5] Ch. Gerth, K. Godehusen, M. Richter, P. Zimmermann, J. Schulz, Ph. Wernet, B. Sonntag, A. G. Kochur, and I. D. Petrov, Phys. Rev. A **61**, 022713 (2000).
[6] A. Penttilä, S. Heinäsmäki, M. Harkoma, S. Fritzsche, R. Sankari, S. Aksela, and H. Aksela, Phys. Rev. A **71**, 022715 (2005).
[7] T. Luhmann, Ch. Gerth, M. Martins, M. Richter, and P. Zimmermann, Phys. Rev. Lett. **76**, 4320 (1996).
[8] E. Kukk, S. Aksela, H. Aksela, O.-P. Sairanen, A. Yagishita, and E. Shigemasa, J. Phys. B **27**, 1965 (1994).
[9] B. Santjer, D. Sundermann, M. Wilmer, and H. Merz, J. Phys. B **30**, 5501 (1997).
[10] O.-P. Sairanen and S. Aksela, J. Phys.: Condens. Matter **4**, 3337 (1992).
[11] M. Bässler, J.-O. Forsell, O. Björneholm, R. Feifel, M. Jurvansuu, S. Aksela, S. Sundin, S. L. Sorensen, R. Nyholm, A. Ausmees, and S. Svensson, J. Electron Spectrosc. Relat. Phenom. **101–103**, 953 (1999); M. Bässler, A. Ausmees, M. Jurvansuu, R. Feifel, J.-O. Forsell, P. de Tarso Fonseca, A. Kivimäki, S. Sundin, S. L. Sorensen, R. Nyholm, O. Björneholm, S. Aksela, and S. Svensson, Nucl. Instrum. Methods Phys. Res. A **469**, 382 (2001).
[12] M. Huttula, S. Heinäsmäki, H. Aksela, E. Kukk, and S. Aksela, J. Electron Spectrosc. Relat. Phenom. **156–158**, 270 (2007).
[13] M. Huttula, K. Jänkälä, A. Mäkinen, H. Aksela, and S. Aksela, New J. Phys. **10**, 013009 (2008).
[14] P. Baltzer, L. Karlsson, M. Lundqvist, and B. Wannberg, Rev. Sci. Instrum. **64**, 2179 (1993).
[15] G. C. King, M. Tronc, F. H. Read, and R. C. Bradford, J. Phys. B **10**, 2479 (1977).
[16] T. X. Carroll, J. D. Bozek, E. Kukk *et al.*, J. Electron Spectrosc. Relat. Phenom. **125**, 127 (2002).
[17] J. Jauhiainen, A. Ausmees, A. Kivimäki, S. J. Osborne, A. Naves de Brito, S. Aksela, S. Svensson, and H. Aksela, J. Electron Spectrosc. Relat. Phenom. **69**, 181 (1994).
[18] F. A. Parpia, C. Froese Fischer, and I. P. Grant, Comput. Phys. Commun. **94**, 249 (1996).
[19] http://physics.nist.gov/PhysRefData/ASD/
[20] M. Huttula, E. Kukk, S. Heinäsmäki, M. Jurvansuu, S. Fritzsche, H. Aksela, and S. Aksela, Phys. Rev. A **69**, 012702 (2004).
[21] A. G. Kochur, V. L. Sukhorukov, and I. D. Petrov, J. Phys. B **29**, 4565 (1996).
[22] J. C. Riviére, F. P. Netzer, G. Rosina, G. Strasser, and J. A. D. Matthew, J. Electron Spectrosc. Relat. Phenom. **36**, 331 (1985).
[23] E. J. McGuire, Sandia Laboratory, Report No. SAND-75–0443, 1975 (unpublished).
[24] H. Aksela, S. Aksela, and H. Pulkkinen, Phys. Rev. A **30**, 865 (1984); A. Kivimäki, L. Pfeiffer, H. Aksela, E. Nõmmiste, and S. Aksela, J. Electron Spectrosc. Relat. Phenom. **101–103**, 43 (1999).
[25] J. Tulkki, Phys. Rev. Lett. **62**, 2817 (1989).
[26] V. Jonauskas, L. Partanen, S. Kučas, R. Karazija, M. Huttula, S. Aksela, and H. Aksela, J. Phys. B **36**, 4403 (2003).